Applied Energy xxx (2012) xxx–xxx

Contents lists available at SciVerse ScienceDirect

Applied Energy

journal homepage: www.elsevier.com/locate/apenergy

Evaluating shortfalls in mixed-integer programming approaches for the optimal design and dispatch of distributed generation systems

Kristopher A. Pruitt [a,*], Robert J. Braun [b], Alexandra M. Newman [a]

[a] Division of Economics and Business, Colorado School of Mines, Golden, CO 80401, USA
[b] Department of Mechanical Engineering, College of Engineering and Computational Sciences, Colorado School of Mines, Golden, CO 80401, USA

HIGHLIGHTS

- We model the optimal design and dispatch of a distributed generation system.
- Our model includes performance characteristics often not considered in simpler models.
- A simpler model underestimates the optimal system capacity compared to our model.

ARTICLE INFO

Article history:
Received 4 April 2012
Received in revised form 12 July 2012
Accepted 20 July 2012
Available online xxxx

Keywords:
Optimization
Mixed-integer nonlinear programming
Distributed generation
Combined heat and power
Fuel cells
Building energy

ABSTRACT

The distributed generation (DG) of combined heat and power (CHP) for commercial buildings is gaining increased interest, yet real-world installations remain limited. This lack of implementation is due, in part, to the challenging economics associated with volatile utility pricing and potentially high system capital costs. Energy technology application analyses are also faced with insufficient knowledge regarding how to appropriately design (i.e., configure and size) and dispatch (i.e., operate) an integrated CHP system. Existing research efforts to determine a minimum-cost-system design and dispatch do not consider many dynamic performance characteristics of generation and storage technologies. Consequently, we present a mixed-integer nonlinear programming (MINLP) model that prescribes a globally minimum cost system design and dispatch, and that includes off-design hardware performance characteristics for CHP and energy storage that are simplified or not considered in other models. Specifically, we model the maximum turn-down, start up, ramping, and part-load efficiency of power generation technologies, and the time-varying temperature of thermal storage technologies. The consideration of these characteristics can be important in applications for which system capacity, building demand, and/or utility guidelines dictate that the dispatch schedule of the devices varies over time. We demonstrate the impact of neglecting system dynamics by comparing the solution prescribed by a simpler, linear model with that of our MINLP for a case study consisting of a large hotel, located in southern Wisconsin, retrofitted with solid-oxide fuel cells (SOFCs) and a hot water storage tank. The simpler model overestimates the SOFC operational costs and, consequently, underestimates the optimal SOFC capacity by 15%.

Published by Elsevier Ltd.

1. Introduction

The on-site generation of heat and power, commonly referred to as distributed generation (DG), is gaining interest in the commercial building sector. A DG system can consist of renewable or non-renewable sources of power generation (e.g., photovoltaic (PV) cells, fuel cells, and other prime movers), electric energy storage (e.g., batteries), heat generation (e.g., heat exchangers and boilers), and/or thermal energy storage (e.g., hot water). For some markets, volatile utility pricing and high technology capital costs reduce the economic viability of DG. However, even in the most economically favorable markets, commercial building application remain limited to uninterrupted or backup power systems. Barriers to widespread adoption of DG at the commercial scale (< 1 MW) can be due to high grid interconnection fees and permitting wait times, as well as the perceived risk in installing new technologies. The lack of DG implementation is also due to the inadequacy of existing tools to determine the optimal configuration, size, and operation of complex, combined heat and power (CHP) systems. We refer to this task of determining the lowest cost mix, capacity, and operational schedule of DG technologies as the design and dispatch problem.

Existing efforts (see [1]) to solve the design and dispatch problem apply techniques that include simulation, evolutionary algorithms (e.g., genetic algorithms), or more traditional

* Corresponding author.
E-mail address: kpruitt@mines.edu (K.A. Pruitt).

0306-2619/$ - see front matter Published by Elsevier Ltd.
http://dx.doi.org/10.1016/j.apenergy.2012.07.030

mathematical programming algorithms (e.g., simplex or branch-and-bound). The leading simulation model in the literature is the Hybrid Optimization Model for Electric Renewables (HOMER) (see [2–5]). HOMER enumerates DG system designs that have sufficient capacity to meet the annual demand of a building of interest, calculates the hourly dispatch associated with each system design, and rank orders the designs based on life-cycle cost. However, the dispatch strategy is pre-specified by the user, rather than determined by the model. The inability to optimally select the system dispatch is particularly troublesome when the system design includes storage, because the model cannot consider the demand in future time periods when choosing the dispatch in the current time period. Thus, as with any simulation model (see also [6–9]), the results are inherently *de*scriptive rather than *pre*scriptive.

Prescriptive models of the design and dispatch problem include variables for the configuration, capacity, and time-varying operation of the technologies in the system. The values of these variables are determined by solving instances of the model with an appropriate algorithm. Evolutionary algorithms (EAs) are applied in a number of studies to determine the dispatch of an existing DG system (see [10,11]) or the design and dispatch of a new system (see [12–14]). Although these studies are capable of prescribing a system design and/or dispatch, the EA approach is fundamentally different than that of more traditional algorithms. In general, search heuristics such as EAs do not include methods for bounding the optimal objective function value and terminate based solely on decreased improvement in the objective. Thus, there is often no way of determining whether the solution which results from the algorithm is close to globally (or even locally) optimal. By contrast, models which apply simplex or branch-and-bound algorithms (see [15–19]) can prescribe a provable, globally optimal system design and dispatch.

Foremost among the global optimization models in the DG literature is the Distributed Energy Resources Customer Adoption Model (DER-CAM) (see [20–23]). DER-CAM is a mixed-integer linear programming (MILP) model that is solved using the branch-and-bound algorithm to determine the number of DG technologies to acquire, along with their operating levels over time, to meet the power and heating demands of a building at minimum capital, operational, and environmental (i.e., emissions) cost. In contrast to other existing research, DER-CAM addresses both the design and dispatch of a DG system, applies a provable global optimization approach, includes both economic and environmental costs in its objective, and considers the generation and storage of both power and heat using renewable and nonrenewable technologies. Given all of these attributes, DER-CAM is the most flexible of the design and dispatch models cited thus far. But, DER-CAM does not consider many performance characteristics that constrain the dynamic (i.e., off-design) operation of DG technologies. Simplifying these characteristics permits a linear formulation of the problem with few integer variable restrictions. Thus, even large instances (i.e., instances possessing long time horizons) of the design and dispatch problem can be solved with relative ease. However, insufficiently modeling the off-design system performance could result in the prescription of unrealistic system dispatch schedules and, ultimately, in the recommendation of a suboptimal system design.

Pruitt et al. [24] address the implementation of higher model fidelity by presenting a mixed-integer nonlinear programming (MINLP) model, referred to as $(\mathcal{P})$, that prescribes a globally minimum cost system design and dispatch, and that includes dynamic[1] performance characteristics of power and heat generation and storage that are simplified or not considered in models such as DER-CAM. In addition to typical constraints on demand, capacity, and inventory balance, $(\mathcal{P})$ models the maximum turn-down, start-up fuel consumption, ramping capability, and part-load electric efficiency of power generation technologies, and models the time-varying temperature of thermal storage technologies. The consideration of these dynamic performance characteristics can be particularly important when the technologies are operated in a load-following (i.e., time-varying), rather than baseload (i.e., fixed), manner. In some applications, the DG system configuration and capacity, the building's energy demands, and/or the local utility's rates, policies, and procedures may require a time-varying dispatch from the DG technologies. In these instances, $(\mathcal{P})$ captures the real-world operation of the technologies more accurately than models which simplify or do not consider dynamic performance characteristics.

The objectives of this work are to: (i) evaluate the differences in optimal design and dispatch when using simplified or higher-fidelity models, (ii) develop insight into when higher-fidelity models are more appropriate to employ than simplified models, and (iii) provide a higher-fidelity model for enabling more detailed engineering analyses of integrated DG systems in building applications.

In this paper, we demonstrate that neglecting system dynamics can result in inaccurate prescriptions of system operation and, subsequently, in suboptimal DG investment. In order to demonstrate this, we present a simplified version of $(\mathcal{P})$, called $(\mathcal{S})$, that does not include maximum turn-down, start up, ramping, or part-load efficiency, and that models thermal storage in terms of energy inventory rather than temperature. The formulation of $(\mathcal{S})$ as a representative model that does not consider system dynamics permits both qualitative and quantitative comparisons with $(\mathcal{P})$. In so doing, we are able to highlight the scenarios for which a more detailed model, such as $(\mathcal{P})$, is preferable to a simpler model, such as $(\mathcal{S})$. The remainder of the paper is organized as follows: Section 2 discusses the specific dynamic performance characteristics considered in our research and their importance given alternative operating strategies. Section 3 provides the MINLP formulation of $(\mathcal{P})$, the MILP formulation of $(\mathcal{S})$, and concludes with an examination of the qualitative differences between $(\mathcal{P})$ and $(\mathcal{S})$. Section 4 demonstrates the numerical impact of the differences between the two formulations with a case study of a representative commercial building application. Finally, Section 5 concludes the paper.

2. System operating strategies

For the DG systems examined in this research, we consider solid-oxide fuel cells (SOFCs) as the primary source of on-site power generation. Thus, one of the goals of solving specific instances of $(\mathcal{P})$ is to determine the appropriate operating strategy (e.g., baseload versus load-following) for the SOFC system. Accurately modeling the operation of DG technologies, such as fuel cells, can require the consideration of a number of performance characteristics. Fuel cells convert the chemical energy of a fuel, such as natural gas, directly into electrical energy through electrochemical reactions. In this way, the performance and technological characteristics of fuel cells resemble those of batteries more than those of conventional, fossil fuel-based combustion generators. However, unlike batteries, fuel cells do not require charging and can continue to produce power as long as they are supplied with reactants (such as fuel and air). The materials of construction employed by SOFCs, in particular, demand high operating temperatures to achieve practical power generating efficiencies. Because SOFCs require a significant amount of time to reach operating temperature (i.e., maximum turn-down), their ability to depart standby mode (i.e., start up) and change power output between time periods (i.e., ramp) is limited (see [25]). Additionally, the ratio of their electric energy output to fuel energy input (i.e., electric efficiency)

[1] The usage of dynamic in this paper refers to both the off-design (or part-load) performance of the SOFC system and the time-dependent thermodynamic state of the water in the storage tank.

Please cite this article in press as: Pruitt KA et al. Evaluating shortfalls in mixed-integer programming approaches for the optimal design and dispatch of distributed generation systems. Appl Energy (2012), http://dx.doi.org/10.1016/j.apenergy.2012.07.030

decreases as power output increases (see [26,27]). Thus, power is generated with greater efficiency at part load (i.e., below maximum power output) than at rated capacity. Maximum turn-down, start-up fuel consumption, power ramping, and part-load electric efficiency are all performance characteristics of off-design SOFC power generation that are modeled in $(\mathcal{P})$.

SOFCs can also be integrated with waste heat recovery and storage to form a CHP system. For instance, the high-temperature exhaust gases from the SOFCs could flow through heat exchangers in a water tank to store thermal energy in the form of hot water. The flowrate of exhaust gas from SOFCs depends on their power output and electric efficiency (see [28]). As power output increases, electric efficiency decreases, and the flowrate of exhaust gas increases. However, the heat that can be applied to the tank depends not only on the flowrate of exhaust gas, but also on the temperature difference between the gas and the tank water. Thus, the time-varying temperature of the water stored in the tank, which is modeled in $(\mathcal{P})$, impacts the effective thermal efficiency of the SOFC system.

The implications for neglecting the dynamic aspects of power and heat generation depend largely on how the SOFC system is operated. Ultimately, the optimal solution to $(\mathcal{P})$ dictates the lowest-cost operating strategy for the system. However, given a specific system configuration, $(\mathcal{P})$ is more likely to select certain operating strategies. In order to illustrate this point, we next discuss the performance limitations of SOFC power and heat dispatch in the context of two operating strategies: baseload and load-following.

2.1. Baseload strategy

Fig. 1 depicts the energy system originally presented in Pruitt et al. [24]. In this system, the power demands of a commercial building are met by the grid (i.e., the local utility) and/or electricity provided by PV cells, SOFCs, and lead-acid batteries. Excess power generated by the PV cells or SOFCs can be charged to the batteries or exported to the grid (i.e., net-metered). Both the space and water heating demands of the building are met by an existing boiler and/or hot water from a storage tank which is heated by exhaust gases from the CHP SOFCs. In this configuration, the SOFCs preheat the water prior to its flow into the boiler, which then ensures the water is delivered to the building's faucets and radiators at the appropriate temperature. The objective of solving the design and dispatch problem is to determine the mix, capacity, and operating strategy of the DG technologies in Fig. 1 that provide the minimum total annual cost.

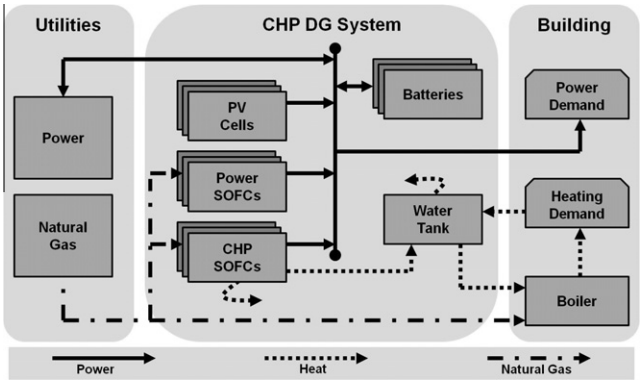

Fig. 1. Combined heat and power (CHP), distributed generation (DG) system consisting of photovoltaic (PV) cells, solid-oxide fuel cells (SOFCs), lead-acid batteries, and a hot water storage tank. This particular system also permits electricity export (i.e., net-metering) to the power utility.

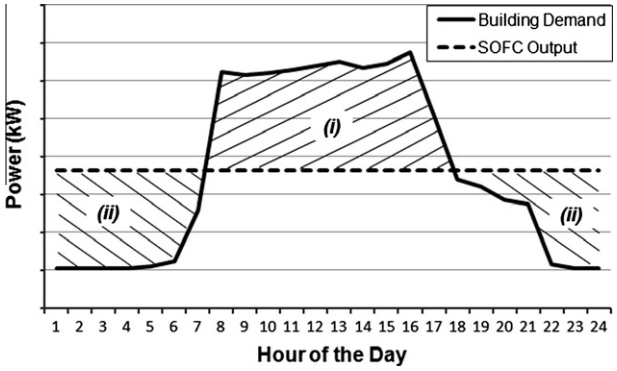

Fig. 2. SOFC power output given a baseload operating strategy. The SOFC output falls short of the building load in periods of high demand (i) and exceeds the building load in periods of low demand (ii).

A robust DG system, such as that in Fig. 1, with multiple sources of electricity import and export, provides flexibility in how the SOFCs are operated. For instance, Fig. 2 depicts an operating strategy for which the SOFCs baseload at their rated (i.e., maximum) capacity. In the region labeled (i), the SOFC power output falls short of the building demand. Consequently, the remaining power demand must be supplied by the PV cells, battery discharge, and/or the grid. The complementary case is demonstrated in the region labeled (ii), where the SOFC power output exceeds the building demand. In (ii), the surplus power generated by the SOFCs must be charged to the batteries or exported to the grid. Thus, a DG system with the technological means to address shortages and surpluses in power supply permits SOFCs the flexibility to operate according to a variety of strategies, including baseloading.

If the SOFC system is baseloaded then limitations on dynamic performance may be of little concern. When baseloading at rated capacity, the SOFCs are rarely turned down to part load or standby, and do not change power or exhaust gas output between time periods. With a fixed exhaust gas input to the storage tank, the heating demand of the building is the only time-varying factor affecting the temperature of the tank water. In this case, the rated power output and efficiency may be the only characteristics required to model the operation of the SOFCs accurately. Thus, in applications for which it is physically possible and economically beneficial to operate the SOFCs in a baseload manner, the system design and dispatch solutions prescribed by $(\mathcal{P})$ may be similar to, if not the same as, solutions prescribed by simpler models that do not consider dynamic performance limitations. However, certain conditions for the DG system and energy market might prevent or discourage baseloading.

2.2. Load-following strategy

Both physical and economic conditions could dictate a decrease in design options compared to the system in Fig. 1. Renewable sources of power, such as PV cells, could have prohibitive capital costs and unpredictable supply. Similarly, high capital costs and charge–discharge inefficiencies could render electricity storage technologies unavailable or unattractive. Finally, local utility net-metering policies or interconnection procedures could discourage or prevent excess power from being exported to the grid. Under these conditions, the DG system has no means of disposing of excess SOFC power and relies solely on the grid to address power shortages. Fig. 3 depicts a system for which PV cells, batteries, and exportation of power to the grid are not viable, and for which, consequently, SOFC baseloading may not be an attractive option.

Please cite this article in press as: Pruitt KA et al. Evaluating shortfalls in mixed-integer programming approaches for the optimal design and dispatch of distributed generation systems. Appl Energy (2012), http://dx.doi.org/10.1016/j.apenergy.2012.07.030

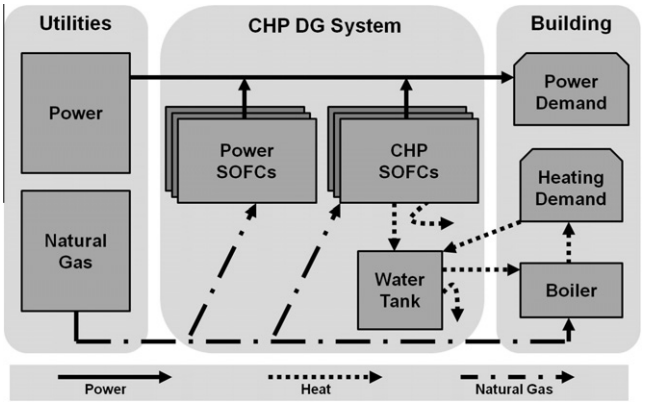

Fig. 3. Combined heat and power (CHP), distributed generation (DG) system consisting of solid-oxide fuel cells (SOFCs) and a hot water storage tank.

With the DG system in Fig. 3, there is far less flexibility in how the SOFC system is operated compared to Fig. 1. This is particularly true when the rated SOFC system capacity is greater than the minimum power load of the building, and the effective price of electricity from the SOFC system is less than that of the utility. In this case, the preferred operating strategy is for the SOFC power output to follow the building load (i.e., load-follow) in all hours for which the demand is less than the rated capacity, as in Fig. 4. In the region labeled (iii), where the building demand exceeds the rated capacity of the SOFCs, the remaining power is provided by the grid. Thus, a DG system with no technological means to address surplus power and only limited means to address power shortages, may force SOFCs to load-follow.

Because load-following requires the SOFCs to operate at off-design power levels, it can be important to consider part-load performance characteristics such as maximum turn-down, start up, ramping, and off-design electric efficiency and exhaust gas output in order to avoid prescribing an unrealistic system dispatch. When SOFCs operate at part load, it is possible that one or more SOFC modules could be forced into standby mode and, therefore, must later start back up when the required power output increases above the maximum turn-down. Also, large increases and decreases in power output throughout the day are constrained to the ramping capability of the SOFC system. As the power output of the SOFCs changes over time, so too do their electric efficiency, their rate of natural gas consumption, and their rate of exhaust gas production. Thus, with load-following, the temperature of the water in the storage tank is determined by both time-varying heat input and output.

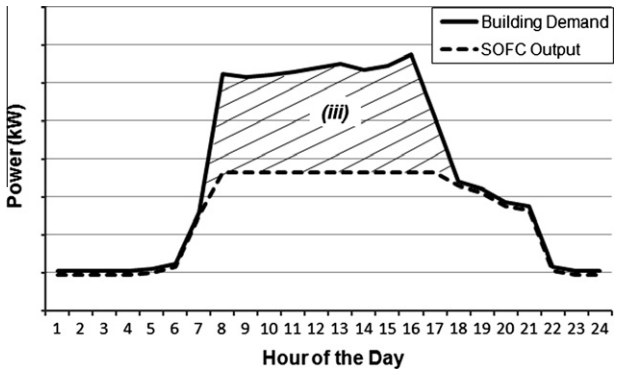

Fig. 4. SOFC power output given a load-following operating strategy. The SOFC output falls short of the building load only in the periods of high demand (iii).

It should be noted that while the focus of the present work is on employing high-temperature SOFC technology, the models and discussion in the following text are applicable to many different prime mover technologies. The desire to have the SOFC system operate in a load-following manner is not unrealistic as long as the temperature constraints are maintained throughout its operating envelope. A recent study suggests that load-following may even be a preferred operating scenario for SOFCs [41].

The aspects of dynamic SOFC operation described above can be critical to realistically modeling the operation of a CHP system in applications that require load-following. However, existing global optimization models of the design and dispatch problem do not consider the maximum turn-down, start-up fuel consumption, ramping capability, and/or part-load electric efficiency of power generators, and/or do not include the quality (i.e., temperature) of stored thermal energy. Simplifying these aspects of system operation allows for a linear formulation of the problem with fewer variables and constraints, but might lead to the prescription of a suboptimal or unrealistic system design and dispatch.

3. Model

In this section, we provide two different mathematical formulations, $(\mathcal{P})$ and $(\mathcal{S})$, of the design and dispatch problem for the system depicted in Fig. 3. Given we address the reduced system, rather than the more complex system depicted in Fig. 1, the $(\mathcal{P})$ formulation presented in this paper contains fewer variables and constraints than that of Pruitt et al. [24]. However, $(\mathcal{P})$ remains a mixed-integer nonlinear program that models off-design performance characteristics of the SOFC system and dynamic characteristics of the water tank, while $(\mathcal{S})$ is a mixed-integer linear program that simplifies or does not include these characteristics. We conclude the section with a discussion of the qualitative differences between the two formulations.

3.1. $(\mathcal{P})$ Formulation

Here we provide the mathematical formulation of $(\mathcal{P})$. Uppercase letters identify variables or sets, while lower-case letters identify parameters or set indices. Superscripts and accents differentiate parameters and variables that use the same base letter. Subscripts distinguish between elements of a set. Some parameters and variables are only defined for certain elements of sets, which are listed in each definition. The units of each parameter and variable are provided in brackets after its definition.

3.1.1. Sets

$j \in \mathcal{J}$: set of all technologies (Consistent with Pruitt et al. [24], we define the elements of $\mathcal{J}$ numerically as 3 = Power SOFC, 4 = CHP SOFC, 5 = Storage Tank, 6 = Boiler.),
$n \in \mathcal{N}$: set of all months,
$t \in \mathcal{T}_n$: set of all hours in month n ($\mathcal{T} = \bigcup_n \mathcal{T}_n$).

3.1.2. Time and demand parameters

δ = demand time increment [hours],
d_t^P, d_t^Q = average power and heating demand, respectively, in hour t [kW] .

3.1.3. Cost and emissions parameters

c_j = amortized capital and install cost of each technology j = 3, 4 [$/kW],
m_j = average O&M cost of each technology j = 3, 4, 6 [$/kW h],

p_t, g_t = price of electricity and natural gas, respectively, from the utility in hour t [$/kW h],
p_n^{max} = peak demand price of power from the utility in month n [$/kW/month],
z = tax on carbon emissions [$/kg],
z^p, z^g = average carbon emissions rate for utility power and gas combustion, respectively [kg/kW h].

3.1.4. Power generation parameters

η_j^{max}, η_j^{min} = max and min, respectively, electric efficiency of each technology j = 3, 4 [fraction],
μ_j = max turn-down of each technology j = 3, 4 [fraction],
σ_j = start-up time for each technology j = 3, 4 to reach operating temperature [hours],
k_j = power output rating of each technology j = 3, 4 [kW],
r_j^{up}, r_j^{down} = max ramp-up and ramp-down rate, respectively, for each technology j = 3, 4 [kW/h].

3.1.5. Heat generation and storage parameters

α_j = average ambient heat loss of water stored in technology j = 5 [fraction],
γ_j = average exhaust gas output from technology j = 4 per unit of fuel input [kg/kW h],
η_j = average thermal efficiency of each technology j = 5, 6 [fraction],
τ_j^{out}, τ_j^{in} = average temperature of fluid out of and into, respectively, each technology j = 4, 5, 6 [°C],
τ^{max}, τ^{min} = max and min, respectively, temperature of water in the system [°C],
h_j = specific heat of fluid output from each technology j = 4, 5 [kW h/(kg °C) or kW h/(gal °C)],
v_j^{max}, v_j^{min} = max and min, respectively, storage capacity of technology j = 5 [gallons].

3.1.6. System design variables

A_j = number of each technology j = 3, 4, 5 acquired [integer],
V_j = water storage capacity of technology j = 5 [gallons].

3.1.7. Power dispatch variables

E_{jt} = electric efficiency of each technology j = 3, 4 operating in hour t [fraction],
N_{jt} = number of each technology j = 3, 4 operating in hour t [integer],
$\acute{N}_{jt}$ = increase in number of each technology j = 3, 4 operating from $t-1$ to t [integer],
P_{jt} = aggregate power output from each technology j = 3, 4 in hour t [kW],
U_t = power purchased from the utility in hour t [kW],
U_n^{max}=max power purchased from the utility in month n [kW].

3.1.8. Heat dispatch and storage variables

B_{jt}^{in} = 1 if water in technology j = 5 is above $\tau_5^{in}+\varepsilon$ at start of hour t, 0 otherwise [binary],
B_{jt}^{out} = 1 if water in technology j = 5 is above τ_6^{out} at start of hour t, 0 otherwise [binary],
F_{jt}^{out} = flowrate of water out of technology j = 5 in hour t [gal/h],
F_{jt}^{in} = flowrate of exhaust gas into technology j = 5 in hour t [kg/h],
G_{jt} = aggregate natural gas input to each technology j = 3, 4, 6 in hour t [kW],
T_{jt} = temperature of water stored in technology j = 5 at the start of hour t [°C].

The objective of $(\mathcal{P})$ minimizes the total capital and operational costs of the system over the time horizon of interest. Objective component (1a) comprises the capital, operations and maintenance (O&M), fuel (start-up and steady-state operation), and emissions costs for the SOFCs. We assume the capital costs for the SOFC-CHP system account for the cost of the waste heat recovery and storage tank integration. Objective component (1b) captures the energy and emissions costs of power purchased from the utility, as well as the O&M, fuel, and emissions costs for the boiler. If SOFCs are not acquired, then the total cost is reduced to component (1b).

Minimize

$$\sum_{j=3,4} c_j k_j A_j + \sum_{j=3,4}\sum_{t\in\mathcal{T}} m_j \delta P_{jt} + \sum_{j=3,4}\sum_{t\in\mathcal{T}} (g_t + z z^g)\left[\frac{\sigma_j \mu_j k_j}{2\eta_j^{min}}\acute{N}_{jt} + \delta G_{jt}\right] \quad (1a)$$

$$+ \sum_{t\in\mathcal{T}} (p_t + z z^p)\delta U_t + \sum_{n\in\mathcal{N}} p_n^{max} U_n^{max} + \sum_{t\in\mathcal{T}} (\eta_6 m_6 + g_t + z z^g)\delta G_{6t} \quad (1b)$$

The constraint set of $(\mathcal{P})$ ensures that the power and heating demands of the building are met, subject to the performance characteristics of the SOFCs, storage tank, and boiler. We provide a brief description of each of the constraints here. See Pruitt et al. [24] for a more detailed discussion of the constraint set.

Constraints (2a)–(2c) address the hourly power and heating demands of the building. Constraint (2a) requires the power demand to be met by the SOFC system and the power purchased from the utility. Constraint (2b) determines the peak power load purchased from the utility in each month. Constraint (2c) dictates that the heating demand be met by the flow of hot water, which must be delivered at a specified temperature. If the water from the storage tank is below the specified delivery temperature (i.e., $B_{5t}^{out}=0$), then the hot water flow from the tank is directly determined by the heating demand. However, if the tank water is above the delivery temperature (i.e., $B_{5t}^{out}=1$), then the hot water flow from the tank is reduced due to the cold water mixing required to achieve the delivery temperature.

$$\sum_{j=3,4} P_{jt} + U_t = d_t^P \quad \forall t \in \mathcal{T} \quad (2a)$$

$$U_n^{max} \geqslant U_t \quad \forall n \in \mathcal{N}, t \in \mathcal{T}_n \quad (2b)$$

$$h_5(\tau_6^{out} - \tau_5^{in})F_{5t}^{out}\left[\left(1 - \left[1 - \frac{\tau_6^{out} - \tau^{min}}{T_{5t} - \tau^{min}}\right]B_{5t}^{out}\right)^{-1}\right] = d_t^Q \quad \forall t \in \mathcal{T} \quad (2c)$$

Constraints (3a) and (3b) account for the design of the thermal storage system. Constraint (3a) ensures that a hot water storage tank is acquired if and only if at least one SOFC -CHP is acquired. Constraint (3b) restricts the selected capacity of the storage tank to the established minimum and maximum based on the building heating load.

$$A_5 \leqslant A_4 \leqslant \left\lceil \frac{\max_{t\in\mathcal{T}}\left\{d_t^P\right\}}{k_4} \right\rceil A_5 \quad (3a)$$

$$v_5^{min} \leqslant V_5 \leqslant v_5^{max} \quad (3b)$$

Constraints (4a)–(4d) address the hourly aggregate power output of the SOFCs. Constraint (4a) dictates that the aggregate power output of the SOFCs must remain between the total output at maximum turn-down and the total output at the nameplate power rating of the SOFCs operating in a given time period. Constraint (4b) limits changes in the aggregate power output from the SOFCs between time periods based on their maximum power ramping capabilities. Constraint (4c) states that the number of SOFCs operating in a given time period cannot exceed the number acquired. Constraint (4d) determines the number of SOFCs that start up between time periods.

Please cite this article in press as: Pruitt KA et al. Evaluating shortfalls in mixed-integer programming approaches for the optimal design and dispatch of distributed generation systems. Appl Energy (2012), http://dx.doi.org/10.1016/j.apenergy.2012.07.030

$$\mu_j k_j N_{jt} \leqslant P_{jt} \leqslant k_j N_{jt} \quad \forall j = 3,\ 4,\ t \in \mathcal{T} \tag{4a}$$

$$-\delta r_j^{\text{down}} N_{jt} \leqslant P_{j,t+1} - P_{jt} \leqslant \delta r_j^{\text{up}} N_{j,t+1} \quad \forall j = 3,\ 4,\ t < |\mathcal{T}| \tag{4b}$$

$$N_{jt} \leqslant A_j \quad \forall j = 3,\ 4,\ t \in \mathcal{T} \tag{4c}$$

$$N_{j,t+1} - N_{jt} \leqslant \acute{N}_{j,t+1} \quad \forall j = 3,\ 4,\ t < |\mathcal{T}| \tag{4d}$$

Constraints (5a)–(5c) relate the energy output and fuel consumption of the technologies in the system. Constraint (5a) defines the electric efficiency of the SOFCs as a decreasing linear function of the share of aggregate power output provided by each operating SOFC. Constraint (5b) establishes the aggregate power output of the SOFCs as the product of the electric efficiency and the aggregate natural gas input. Constraint (5c) dictates that the heat output from the boiler, which depends on the temperature and flowrate of hot water from the storage tank, must be equivalent to the product of the boiler's thermal efficiency and natural gas consumption.

$$E_{jt} = \left(\frac{\eta_j^{\max} - \mu_j \eta_j^{\min}}{1 - \mu_j}\right) - \left(\frac{\eta_j^{\max} - \eta_j^{\min}}{k_j(1 - \mu_j)}\right)\left(\frac{P_{jt}}{N_{jt}}\right) \quad \forall j = 3,\ 4,\ t \in \mathcal{T} \tag{5a}$$

$$E_{jt} G_{jt} = P_{jt} \quad \forall j = 3,\ 4,\ t \in \mathcal{T} \tag{5b}$$

$$\eta_6 G_{6t} = h_5 F_{5t}^{\text{out}} (\tau_6^{\text{out}} - T_{5t})(1 - B_{5t}^{\text{out}}) \quad \forall t \in \mathcal{T} \tag{5c}$$

Constraint (6a) limits the flowrate of hot exhaust gas into the storage tank to the maximum flowrate of exhaust gas out of the CHP SOFCs.

$$F_{5t}^{\text{in}} \leqslant \gamma_4 G_{4t} \quad \forall t \in \mathcal{T} \tag{6a}$$

Constraints (7a)–(7e) address the storage of thermal energy in the form of hot water. Constraint (7a) states that the change in storage tank water temperature between time periods, including ambient heat loss, is calculated as the quotient of the net thermal energy added to the tank and the heat capacity of the water volume. The net thermal energy added to the tank (i.e., the numerator of the quotient on the right-hand side of the constraint) is calculated as the difference between the thermal energy added by the SOFCs, after considering the efficiency of the heat exchange, and the thermal energy removed for the building heating demand. In both cases, thermal energy is calculated as the product of the time increment, specific heat capacity, flowrate, and temperature difference. Constraint (7b) reduces the temperature of the water flowing into the boiler to the average return temperature if a storage tank is not acquired. Constraint (7c) determines the value of the binary variable that controls the tank water's ambient heat loss. Constraint (7d) determines the value of the binary variable that controls the need for additional heating from the boiler. Constraint (7e) dictates that the temperature of the water at the end of the time horizon must be equivalent to the water temperature at the beginning of the time horizon.

$$T_{5,t+1} - (1 - \alpha_5 B_{5t}^{\text{in}}) T_{5t} = \frac{\delta \eta_5 h_4 F_{5t}^{\text{in}} (\tau_4^{\text{out}} - T_{5t}) - \delta h_5 F_{5t}^{\text{out}} (T_{5t} - \tau_5^{\text{in}})}{h_5 V_5} \quad \forall t < |\mathcal{T}| \tag{7a}$$

$$T_{5t} - \tau_5^{\text{in}} \leqslant (\tau^{\max} - \tau_5^{\text{in}}) A_5 \quad \forall t \in \mathcal{T} \tag{7b}$$

$$\varepsilon B_{5t}^{\text{in}} \leqslant T_{5t} - \tau_5^{\text{in}} \leqslant \varepsilon + (\tau^{\max} - \tau_5^{\text{in}} - \varepsilon) B_{5t}^{\text{in}} \quad \forall t \in \mathcal{T} \tag{7c}$$

$$(\tau_5^{\text{in}} - \tau_6^{\text{out}})(1 - B_{5t}^{\text{out}}) \leqslant T_{5t} - \tau_6^{\text{out}} \leqslant (\tau^{\max} - \tau_6^{\text{out}}) B_{5t}^{\text{out}} \quad \forall t \in \mathcal{T} \tag{7d}$$

$$T_{5,1} = T_{5,|\mathcal{T}|} \tag{7e}$$

Constraints (8a)–(8d) establish the non-negativity and integrality of the variables, as appropriate.

$$U_t,\ P_{jt},\ \acute{N}_{jt},\ E_{jt},\ G_{jt},\ F_{jt}^{\text{out}},\ F_{jt}^{\text{in}},\ T_{jt},\ V_j \geqslant 0 \quad \forall j \in \mathcal{J},\ t \in \mathcal{T} \tag{8a}$$

$$U_n^{\max} \geqslant 0 \quad \forall n \in \mathcal{N} \tag{8b}$$

$$A_j, N_{jt} \geqslant 0,\ \text{integer} \quad \forall j = 3,\ 4,\ t \in \mathcal{T} \tag{8c}$$

$$A_j, B_{jt}^{\text{in}}, B_{jt}^{\text{out}} \quad \text{binary} \quad \forall j = 5,\ t \in \mathcal{T} \tag{8d}$$

The $(\mathcal{P})$ formulation includes a linear objective, $17|\mathcal{T}| + |\mathcal{N}| + 4$ variables ($2|\mathcal{T}| + 2$ general integer, $2|\mathcal{T}| + 1$ binary), and $27|\mathcal{T}| - 2$ constraints ($7|\mathcal{T}| - 1$ nonlinear). All of the nonlinearities in $(\mathcal{P})$ consist of nonlinear equality constraints (see (2c), (5a)–(5c) and (7a)). Thus, the constraint set is nonconvex. Given the difficulties associated with solving nonconvex MINLPs, Pruitt et al. [24] introduce specialized convexification and linearization techniques for solving large instances of $(\mathcal{P})$ whose solutions exceed the capability of existing solvers.

3.2. $(\mathcal{S})$ Formulation

In this section, we present a simpler formulation, $(\mathcal{S})$, of the design and dispatch problem which does not consider maximum turn-down, start up, ramping, part-load efficiency, and thermal storage temperature. We formulate $(\mathcal{S})$ as a representative model that simplifies system dynamics so that we may evaluate the qualitative and quantitative impacts of not using a more detailed model like $(\mathcal{P})$. We introduce the objective and constraints of $(\mathcal{S})$ briefly here and provide a more thorough discussion of how they differ from those of $(\mathcal{P})$ in Section 3.3. $(\mathcal{S})$ requires the definition of the following additional parameters and variables:

3.2.1. Parameters

$\eta_j^P,\ \eta_j^Q$ = rated electric and thermal efficiency, respectively, of each technology $j = 3, 4$ [fraction],

s_j = thermal storage capacity of technology $j = 5$ [kW h].

3.2.2. Variables

Q_{jt} = inventory of thermal energy stored in technology $j = 5$ at the start of hour t [kW h],

$Q_{jt}^{\text{out}},\ Q_{jt}^{\text{in}}$ = heat output from and input to, respectively, each technology $j = 5, 6$ in hour t [kW].

Minimum total cost

Minimize

$$\sum_{j=3,4} c_j k_j A_j + \sum_{j=3,4} \sum_{t \in \mathcal{T}} m_j \delta P_{jt} + \sum_{j=3,4} \sum_{t \in \mathcal{T}} (g_t + z z^g) \delta G_{jt} \tag{9a}$$

$$+ \sum_{t \in \mathcal{T}} (p_t + z z^p) \delta U_t + \sum_{n \in \mathcal{N}} p_n^{\max} U_n^{\max} + \sum_{t \in \mathcal{T}} (\eta_6 m_6 + g_t + z z^g) \delta G_{6t} \tag{9b}$$

subject to

Power and heat demand

$$\sum_{j=3,4} P_{jt} + U_t = d_t^P \quad \forall t \in \mathcal{T} \tag{10a}$$

$$U_n^{\max} \geqslant U_t \quad \forall n \in \mathcal{N},\ t \in \mathcal{T}_n \tag{10b}$$

$$Q_{5t}^{\text{out}} + Q_{6t}^{\text{out}} = d_t^Q \quad \forall t \in \mathcal{T} \tag{10c}$$

System acquisition

$$A_5 \leqslant A_4 \leqslant \left\lceil \frac{\max_{t \in \mathcal{T}} \left\{ d_t^P \right\}}{k_4} \right\rceil A_5 \tag{11a}$$

Power generation

$$P_{jt} \leqslant k_j A_j \quad \forall j = 3,\ 4,\ t \in \mathcal{T} \tag{12a}$$

Natural gas consumption

$$\eta_j^P G_{jt} = P_{jt} \quad \forall j = 3,\ 4,\ t \in \mathcal{T} \tag{13a}$$

$$\eta_6 G_{6t} = Q_{6t}^{\text{out}} \quad \forall t \in \mathcal{T} \tag{13b}$$

Heat generation

$$Q_{5t}^{\text{in}} \leqslant \eta_4^Q G_{4t} \quad \forall t \in \mathcal{T} \tag{14a}$$

Heat storage

$$Q_{5,t+1} - (1-\alpha_5)Q_{5t} = \delta\left(\eta_5 Q_{5t}^{\text{in}} - Q_{5t}^{\text{out}}\right) \quad \forall t < |\mathcal{T}| \tag{15a}$$

$$Q_{5t} \leqslant s_5 A_5 \quad \forall t \in \mathcal{T} \tag{15b}$$

$$Q_{5,1} = Q_{5,|\mathcal{T}|} \tag{15c}$$

Non-negativity and integrality

$$U_t,\ P_{jt},\ G_{jt},\ Q_{jt},\ Q_{jt}^{\text{out}},\ Q_{jt}^{\text{in}} \geqslant 0 \quad \forall j \in \mathcal{J},\ t \in \mathcal{T} \tag{16a}$$

$$U_n^{\max} \geqslant 0 \quad \forall n \in \mathcal{N} \tag{16b}$$

$$A_j \geqslant 0, \quad \text{integer} \quad \forall j = 3,\ 4 \tag{16c}$$

$$A_j \quad \text{binary} \quad \forall j = 5 \tag{16d}$$

The ($\mathcal{S}$) formulation has a linear objective, and includes $7|\mathcal{T}|+1$ fewer variables and $16|\mathcal{T}|-4$ fewer constraints than ($\mathcal{P}$). Additionally, ($\mathcal{S}$) contains only two general integer variables, one binary variable, and is comprised of only linear constraints. With only three total integer variables and a linear (i.e., convex) constraint set, instances of ($\mathcal{S}$) are much simpler to solve than those of ($\mathcal{P}$).

3.3. Differences between ($\mathcal{P}$) and ($\mathcal{S}$)

Qualitatively, ($\mathcal{P}$) and ($\mathcal{S}$) differ in how they model the generation of power and heat by the SOFC system, and the storage of heat in the water tank. In terms of power generation, ($\mathcal{P}$) and ($\mathcal{S}$) differ in how they model (i) the maximum turn-down, (ii) the fuel consumption, (iii) the start up, and (iv) the ramping limitations of the SOFCs. In terms of heat generation and storage, ($\mathcal{P}$) and ($\mathcal{S}$) differ in how they model (v) the heat charged to, (vi) the heat discharged from, and (vii) the capacity of the water tank. In this subsection, we provide a detailed discussion of these seven qualitative differences. We then examine the quantitative impact of the modeling differences in Section 4.

3.3.1. Power generation

An examination of SOFC natural gas consumption at various power output levels highlights the differences in how ($\mathcal{P}$) and ($\mathcal{S}$) model power generation. Fig. 5 depicts the hourly natural gas consumption of a representative SOFC as a function of its power output.

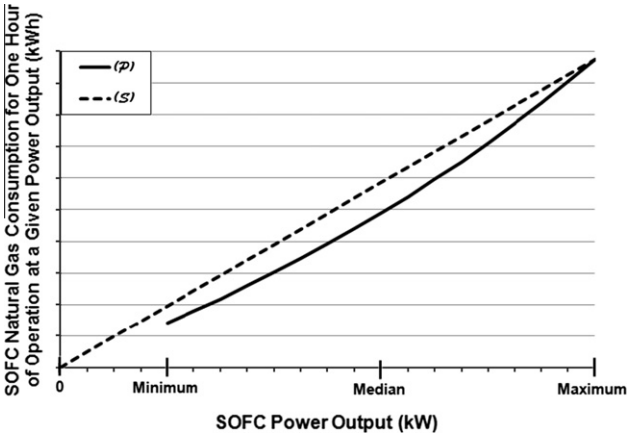

Fig. 5. Comparison of SOFC natural gas consumption at minimum, median, and maximum power output as modeled in ($\mathcal{P}$) versus ($\mathcal{S}$).

In ($\mathcal{P}$), the left-hand side of constraint (4a) enforces a minimum power output for the SOFCs that are operating (i.e., not in standby mode) in a given time period. Given the minimum operating temperature required for power generation, SOFCs cannot operate at power levels below this maximum turn-down. Thus, the range of power output levels below the maximum turn-down (i.e., between zero and minimum power output) is appropriately restricted in ($\mathcal{P}$). However, because constraint (12a) in ($\mathcal{S}$) does not include the operational status and maximum turn-down of the SOFCs, power dispatch solutions (i.e., prescribed values for P_{jt}) are permitted to select output levels below the maximum turn-down (as depicted in Fig. 5). Such solutions cannot be implemented in practice.

Constraints (4a) and (4c) in ($\mathcal{P}$) and constraint (12a) in ($\mathcal{S}$) similarly limit the maximum aggregate power output of the SOFCs to the total nameplate power rating of the SOFCs that are acquired. Furthermore, because ($\mathcal{S}$) fixes the electric efficiency of the SOFCs to the rated efficiency (i.e., the efficiency at nameplate power output), the natural gas consumption at maximum power output is the same as in ($\mathcal{P}$). However, the natural gas consumption of the SOFCs at part-load differs between the two formulations. In ($\mathcal{P}$), constraints (5a) and (5b) dictate that natural gas consumption decreases nonlinearly as power output decreases. By contrast, constraint (13a) in ($\mathcal{S}$) indicates that natural gas consumption decreases linearly as power output decreases. The result of these differences is that ($\mathcal{S}$) overestimates the fuel consumption whenever the SOFCs operate at part-load (as depicted in Fig. 5). Thus, when SOFCs load-follow, the time-varying electric efficiency captured in ($\mathcal{P}$) allows for a more accurate calculation of fuel consumption.

The overestimation of SOFC fuel consumption in ($\mathcal{S}$) is partially offset in time periods in which a positive number of SOFCs start up. In ($\mathcal{P}$), the variable $\acute{N}_{jt}$ found in objective component (1a) and constraint (4d) enforces a fuel requirement for the SOFCs to depart standby mode and achieve operating temperature. If a SOFC's operational status changes from "standby" to "on" between successive time periods, then the objective accounts for the cost associated with the natural gas consumed by the SOFC to achieve the maximum turn-down. We calculate the gas required for start up by assuming a SOFC requires σ_j hours to increase power from zero to $\mu_j k_j$, and that fuel is consumed during start up with the same efficiency $\eta_j^{\min}$ as at rated capacity. However, objective component (9a) in ($\mathcal{S}$) does not account for the fuel required for SOFC start up, nor do any constraints. Thus, in ($\mathcal{S}$), the underestimation of start-up fuel consumption partially offsets the overestimation of steady-state fuel consumption in any hour in which SOFCs start up.

Another key difference in how ($\mathcal{P}$) and ($\mathcal{S}$) model power generation pertains to the ramping capability of the SOFCs. In ($\mathcal{P}$), ramping is explicitly limited in constraint (4b), which we restate here:

$$-\delta r_j^{\text{down}} N_{jt} \leqslant P_{j,t+1} - P_{jt} \leqslant \delta r_j^{\text{up}} N_{j,t+1} \quad \forall j = 3,\ 4,\ t < |\mathcal{T}|.$$

On the other hand, ($\mathcal{S}$) only implicitly restricts changes in SOFC power output. Based on constraints (12a) and (16a), we can derive the following ramping restrictions:

$$-k_j A_j \leqslant P_{j,t+1} - P_{jt} \leqslant k_j A_j \quad \forall j = 3,\ 4,\ t < |\mathcal{T}|. \tag{17}$$

Eq. (17) indicates that, in ($\mathcal{S}$), SOFC power output is permitted to increase or decrease by the aggregate nameplate power rating of the SOFCs that are acquired. However, depending on the demand time increment and the number of operational SOFCs, a ramp (i.e., $P_{j,t+1} - P_{jt}$) of this magnitude may not be achievable. Constraint (4b) in ($\mathcal{P}$) accounts for this ramping limitation. If $-\delta r_j^{\text{down}} N_{jt} > -k_j A_j$ or $\delta r_j^{\text{up}} N_{j,t+1} < k_j A_j$ in a given time period, then ($\mathcal{P}$) provides

tighter restrictions on SOFC ramping than ($\mathcal{S}$) does. Furthermore, the consideration of sub-hourly power demand (i.e., $\delta < 1$) and SOFC standby mode (i.e., $N_{jt} < A_j$) increase the likelihood that ($\mathcal{S}$) overestimates the ramping capacity. This situation could result in ($\mathcal{S}$) prescribing dispatch schedules that cannot be implemented in a given application.

3.3.2. Heat generation and storage

In addition to the differences in modeling power generation, ($\mathcal{P}$) and ($\mathcal{S}$) differ in how they account for the generation and storage of heat. The most fundamental difference is how heat itself is represented in the two formulations. In ($\mathcal{S}$), the flow of heat is represented directly by the variables Q_{jt}^{out} and Q_{jt}^{in}, and the amount of thermal energy stored is represented by Q_{jt}. In ($\mathcal{P}$), however, heat (or thermal energy) is determined as the product of a fluid's specific heat capacity, flowrate (or volume), and temperature change. This alternative representation of heat and thermal energy permits the consideration of more detailed performance characteristics of thermal systems. Specifically, the heat charged to and discharged from the storage tank can be modeled as a function of the flowrate and temperature of the exhaust gas supplied by the SOFCs and the hot water demanded by the building.

Fig. 6 depicts the maximum thermal energy that can be charged to the storage tank in an hour by the exhaust gas from a representative SOFC operating at minimum, median, and maximum power output. In ($\mathcal{S}$), the thermal energy that can be added to the storage tank by SOFC exhaust gas is independent of the temperature of the water in the tank, and is based solely on the rated thermal efficiency of the SOFC (see constraints (14a) and (15a)). As a result, the maximum thermal energy that can be charged to the tank is fixed for a given SOFC power output (as demonstrated in Fig. 6). Conversely, in ($\mathcal{P}$), the thermal energy that can be added to the tank is directly determined by the temperature of the tank water (see constraints (6a) and (7a)). The greater the temperature differential between the SOFC exhaust gas and the tank water, the greater the amount of thermal energy that can be recovered and stored in the tank. Consequently, the maximum thermal energy that can be added to the tank decreases as the water temperature increases (as demonstrated in Fig. 6). In general, these differences between the two formulations result in ($\mathcal{S}$) overestimating the amount of heat that can be charged to the storage tank. However, when the tank water is below delivery temperature and SOFC power output is at or near its maximum, ($\mathcal{S}$) underestimates the available heat.

Accounting for water temperature also leads to differences in how ($\mathcal{P}$) and ($\mathcal{S}$) model the tank discharge. Fig. 7 presents the

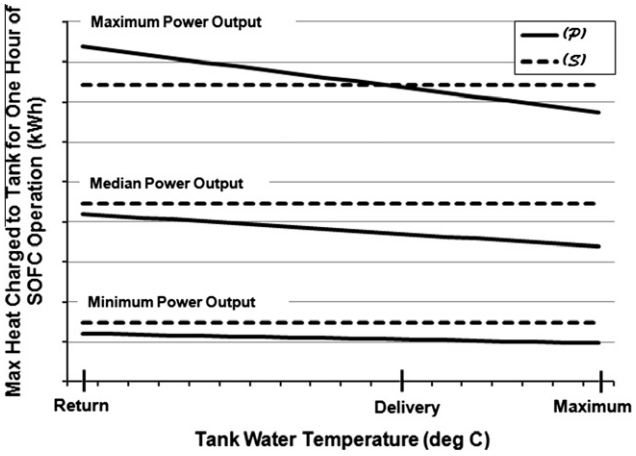

Fig. 6. Comparison of heat charged to storage tank for SOFC operating at minimum, median, and maximum power output as modeled in ($\mathcal{P}$) versus ($\mathcal{S}$).

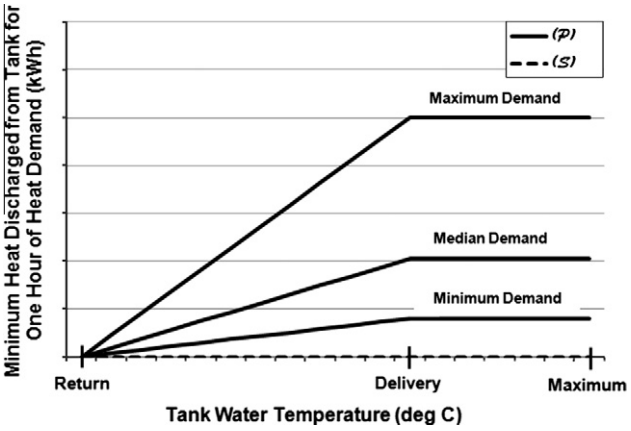

Fig. 7. Comparison of heat discharged from storage tank to meet minimum, median, and maximum demands as modeled in ($\mathcal{P}$) versus ($\mathcal{S}$).

minimum thermal energy that must be discharged from the storage tank in an hour to meet representative minimum, median, and maximum demands. In ($\mathcal{S}$), there is no minimum requirement on the portion of heating demand that must be met by the storage tank (see constraints (10c) and (15a)). Thus, the tank is permitted to provide as little as zero kilowatt-hours of thermal energy (as depicted in Fig. 7) or as much as the full inventory of stored energy in the tank, regardless of the water temperature. By contrast, constraints (2c) and (7a) in ($\mathcal{P}$) enforce a minimum provision of heat by the storage tank whenever the tank water temperature is above the average return temperature. For hours in which the tank water is between the return and delivery temperatures (as determined by constraints (7c) and (7d)), the storage tank provides a positive flow of hot water (and thus heat), with the boiler providing the remaining heat required to deliver the water (see constraint (5c)). As the tank water temperature increases, the portion of heating demand met by the storage tank increases (as depicted in Fig. 7), and the portion met by the boiler decreases. For hours in which the tank water is at or above delivery temperature, *all* of the heating demand is met by the storage tank. In this case, no additional heating is required by the boiler. Thus, for hours in which both the tank water temperature and heating demand are high, ($\mathcal{S}$) likely underestimates the portion of demand met by the storage tank. However, in periods of lower heating demand and water temperature, it is possible for ($\mathcal{S}$) to overestimate the tank heat discharge.

For the representative cases demonstrated in Figs. 6 and 7, the net result of the limitations on tank heat charge and discharge is that the time-varying inventory of stored thermal energy is more accurately modeled in ($\mathcal{P}$) versus ($\mathcal{S}$). This is particularly true when the SOFC power output and building heating demand are high. When SOFC power output is at its maximum, the slope of the ($\mathcal{P}$)-line in Fig. 6 is at its greatest (in absolute value). The same is true of the slope of the ($\mathcal{P}$)-line in Fig. 7 when the heating demand is at its maximum. Due to the steep slopes of these lines, the thermal energy charged to or discharged from the storage tank is more sensitive to changes in the water temperature compared to when SOFC power output and heating demand are low. This sensitivity can lead to wild fluctuations in the thermal energy available from the tank. Because the limits on maximum charge and minimum discharge in ($\mathcal{S}$) are independent of the tank water temperature, ($\mathcal{S}$) is less capable of capturing these fluctuations in available thermal energy. As a result, there exist instances for which ($\mathcal{S}$) inaccurately represents the operation of the tank.

The final difference between ($\mathcal{P}$) and ($\mathcal{S}$) concerns the way in which the two formulations model the capacity of the thermal storage device. In ($\mathcal{S}$), the maximum allowable inventory of thermal

Please cite this article in press as: Pruitt KA et al. Evaluating shortfalls in mixed-integer programming approaches for the optimal design and dispatch of distributed generation systems. Appl Energy (2012), http://dx.doi.org/10.1016/j.apenergy.2012.07.030

energy in the storage tank (i.e., the tank size) is a fixed parameter s_5 (see constraint (15b)), the value of which is selected by the user a priori. Alternatively, $(\mathcal{P})$ models the tank size as a variable V_5 (see constraint (3b)), the value of which is optimally selected by the solution algorithm. When modeling the temperature and flowrate of fluids into and out of the tank, the size of the tank determines the increase or decrease in stored thermal energy. Thus, $(\mathcal{P})$ optimally sizes the storage device based on the heat supplied by the SOFCs and the heat demanded by the building.

4. Case study

In this section, we contrast solutions from $(\mathcal{P})$ and $(\mathcal{S})$ for a six-story, 122,000 square foot hotel located in southern Wisconsin. The power and heating loads for this building type, and the local utility rates, policies, and procedures, encourage the load-following behavior by the SOFCs previously discussed in Section 2.2. Hence, this scenario highlights the deficiencies exhibited by $(\mathcal{S})$ in modeling dynamic performance. We first present the building, utility, and technology parameter values applied in the case study, and then provide the results from solving $(\mathcal{P})$ and $(\mathcal{S})$.

4.1. Building, utility, and technology data

In this section, we provide the values assigned to the parameters defined in Section 3.1 for this particular case study. The hourly ($\delta = 1$) power and heating demands (d_t^P and d_t^Q) are simulated in EnergyPlus (see [29]) using a Department of Energy commercial reference building model (see [30]). The power demand, which averages 142 kW, includes lighting, equipment, and cooling, while the heating demand, which averages 256 kW, includes both space and water heating. The hotel's hourly demands on a representative summer day are depicted in Fig. 8.

The average electricity and natural gas prices listed in Table 1 are based on Wisconsin Electric Power Company's rate schedule for general commercial service (see [31]) and Wisconsin Electric-Gas Operations' rate schedule for firm sales service (see [32]). These energy charges are also consistent with statistics reported by the Energy Information Administration (EIA) for the state of Wisconsin (see [33,34]). The aforementioned EIA reports additionally provide the basis for our calculation of the Wisconsin electric industry's average rate of carbon emissions.

According to the Network for New Energy Choices (NNEC), the state of Wisconsin's net-metering policies and interconnection procedures discourage customer-sited DG (see [35]). The NNEC cites Wisconsin Public Service Commission standards which limit DG system capacity, restrict customer energy credits, require excessive customer insurance, and include hidden interconnection fees. The standard with the greatest impact on the SOFC system design is a 20 kW maximum DG system capacity. As we demonstrate in the numerical results, the optimal DG system capacity for the large hotel is much greater than 20 kW. Because the DG system exceeds the allowable capacity, net-metering is not permitted, and the SOFCs have no means to dispose of excess power.

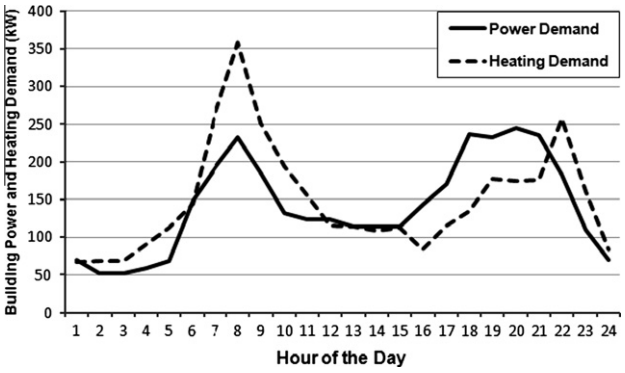

Fig. 8. Power and heating demands on a summer day for a large hotel located in southern Wisconsin.

Table 1
Cost, emissions, and technology parameter values applied in the case study.

Parameter	Value	Units
p_t, g_t $\forall t$	0.10, 0.03	\$/kW h
$p_n^{\max}$ $\forall n$	6.00	\$/kW/month
z	0.02	\$/kg
z^P, z^g	0.74, 0.18	kg/kW h
c_3, c_4	226, 271	\$/kW/year
m_3, m_4, m_6	0.020, 0.024, 0.010	\$/kW h
k_3, k_4	10, 10	kW
σ_3, σ_4	2, 2	hours
μ_3, μ_4	0.2, 0.2	n/a
r_3^{up}, r_4^{up}, r_3^{down}, r_4^{down}	4, 4, 4, 4	kW/hour
$\eta_3^{\max}$, $\eta_4^{\max}$, $\eta_3^{\min}$, $\eta_4^{\min}$	0.57, 0.57, 0.41, 0.41	HHV-basis
$v_5^{\max}$, $v_5^{\min}$	4200, 1000	gallons
η_5, η_6	0.80, 0.75	n/a
α_5	0.01	n/a
γ_4	2.05	kg/kW h
h_4	0.0003	kW h/(kg °C)
h_5	0.004	kW h/(gal °C)
τ_4^{out}, τ_5^{in}, τ_6^{out}	365, 20, 60	°C
$\tau^{\max}$, $\tau^{\min}$	85, 15	°C

The costs and performance characteristics of the SOFCs and water tank are listed in Table 1. The annualized capital and installation costs for the SOFCs applied here are lower than those typically reported in the current literature. At present, the uninstalled unit cost of stationary commercial SOFC systems intended for building applications ranges from \$4000/kW to \$47,500/kW depending on the system size, annual production level, and specific type of SOFC technology (e.g., tubular or planar stacks) (see [36–38]). Furthermore, the additional costs associated with the installation of SOFC systems can be as much as the capital cost. However, we find that, without subsidies, costs of this magnitude result in both $(\mathcal{P})$ and $(\mathcal{S})$ choosing the grid-only solution (i.e., no SOFCs acquired). Thus, the initial capital and installation cost used for the SOFCs in this case study is \$1,600/kW. The cost increase above this value for CHP integration, including the water tank, is 20%. The initial cost is continuously compounded at 5% interest over a 15-year system lifetime to obtain a lifetime opportunity cost, which is then divided by the 15 years to determine the annual costs (c_3 and c_4) reported in Table 1. We assume these reduced annual costs in the case study in order to induce DG acquisition according to both $(\mathcal{P})$ and $(\mathcal{S})$, thereby providing a means to contrast the system design and dispatch selected by the two formulations. However, significant cost reduction is anticipated as the technology matures and production volumes of 50,000 per year or more are reached. Projected system capital costs of current, state-of-the-art SOFC technology as reported by leading developers is expected to be in the \$800/kW range for MW-scale systems (see [39]).

Each of the performance characteristics of the SOFCs and water tank listed in the table are captured in $(\mathcal{P})$. On the other hand, $(\mathcal{S})$ does not include the maximum turn-down, start up, ramping, and part-load efficiency of the SOFCs, and does not consider the temperature of the water in the storage tank. Given these exclusions, $(\mathcal{S})$ simply models the operation of the SOFCs with the rated power output (k_j), and rated electric and thermal efficiencies $\left(\eta_j^P, \eta_j^Q\right)$ of 0.41 and 0.19, respectively, on a higher heating value (HHV) basis. These efficiencies are consistent with the SOFCs operating at

maximum power output and the exhaust heat transferring to tank water at delivery temperature. The thermal efficiency of 0.19 is calculated based on constraints (6a) and (7a), using the formula $\gamma_4 h_4(\tau_4^{out} - \tau_6^{out})$ and the specific parameter values in Table 1. In $(\mathcal{S})$, the fixed storage capacity (s_5) of the tank is expressed in terms of thermal energy, rather than water volume, and is set to a value equivalent to the maximum hourly heating load (1086 kW h) for the year. This capacity is consistent with the upper bound on tank volume in $(\mathcal{P})$, given the maximum allowable temperature of the water.

4.2. Numerical results

Here we present the optimal system design and dispatch prescribed by $(\mathcal{P})$ and $(\mathcal{S})$ for the hotel, based on a typical year's hourly demand (8760 h). Both formulations are coded in AMPL Version 20090327 and solved with CPLEX 12.3 (see [40]) on a 64-bit Linux workstation with four 2.27 GHz Intel processors and 12 GB of RAM. Given the nonlinear nature of $(\mathcal{P})$, we apply heuristic linearization techniques to determine integer-feasible solutions and implement convex underestimation to determine the proximity of those solutions to global optimality (see [24]). For the 1-year instances presented here, the linearization heuristic provides an integer-feasible solution to $(\mathcal{P})$ in 3–4 s. However, the convex underestimation problem requires significantly longer solve times (greater than 10 h) to bound the integer-feasible solutions to within close proximity (less than 10%) of global optimality. On the other hand, 1-year instances of $(\mathcal{S})$ solve to within 1% of global optimality in 1–2 s. Although $(\mathcal{S})$ provides the possibility of significantly shorter solve times, the trade-off is the prescription of a suboptimal system design and an infeasible system dispatch.

The optimal system design and dispatch determined by $(\mathcal{P})$ includes 130 kW of on-site capacity (represented as 13×10 kW SOFC-CHP modules), sizes a single water storage tank to 3900 gal, and operates the SOFC system in a load-following manner. Based on the maximum allowable water temperature of 85 °C and the average return temperature of 20 °C, the 3900 gal tank has a maximum thermal energy capacity of roughly 1014 kW h. By contrast, the design and dispatch prescribed by $(\mathcal{S})$ consists of only 110 kW of capacity (11 SOFC-CHP modules), sizes the tank to the pre-determined 1086 kW h, and still operates the SOFC system in a load-following manner.

Annual statistics for the optimal system design and dispatch determined by $(\mathcal{P})$ are listed in the second column of Table 2, while the same statistics for $(\mathcal{S})$ are listed in the third column. The system design and dispatch prescribed by both formulations afford a total annual cost less than the cost ($284,767) incurred by the grid and boiler alone. However, the total annual cost (including capital *and* operational costs) for the 13 SOFC system determined by $(\mathcal{P})$ is *less* than the total annual cost of the 11 SOFC system determined by $(\mathcal{S})$.

The suboptimal system design determined by $(\mathcal{S})$ results from its inability to consider the dynamic performance of the SOFCs and water tank as part of the system dispatch. Specifically, neglecting power ramping limitations, part-load electric efficiency, and thermal storage temperature causes $(\mathcal{S})$ to overestimate the total annual operational (i.e., utility gas, utility power, and O&M) cost of the system. We demonstrate this with the statistics listed in the fourth and fifth columns of Table 2. In the fourth column of the table, we fix the system design to the 110 kW system selected by $(\mathcal{S})$ and solve $(\mathcal{P})$ to determine the system dispatch. Even though the system designs, and thus the investment costs, in the third and fourth columns of the table are the same, the system dispatches, and thus the operational costs, are different. The $(\mathcal{S})$ dispatch overestimates the total annual operational cost compared to $(\mathcal{P})$. Similarly, in the fifth column of the table, we fix the system design to the 130 kW system selected by $(\mathcal{P})$ and solve $(\mathcal{S})$ to determine the system dispatch. Again, the total annual operational cost in the fifth column is greater than that in the second column, even though the annual investment costs are identical. Although these differences in operational costs between $(\mathcal{P})$ and $(\mathcal{S})$ are relatively small, the overestimation of total annual cost is enough to cause $(\mathcal{S})$ to favor the smaller (110 kW) system capacity when the larger (130 kW) system capacity is not fixed. Thus, not considering the dynamic performance characteristics of the DG technologies causes $(\mathcal{S})$ to undersize the system capacity by 15% compared to $(\mathcal{P})$.

The annual summary statistics listed in Table 2 demonstrate the cumulative effect of not considering power ramping limitations, part-load electric efficiency, and thermal storage temperature. However, a more detailed examination of the *hourly* system dispatch is required to reveal the source of the $(\mathcal{S})$ formulation's tendency to overestimate the total annual operational costs. Thus, we next compare the dispatches dictated by $(\mathcal{P})$ and $(\mathcal{S})$ over a single 24-h period for the 130 kW system. Using the same annual data that is summarized in the second and fifth columns of Table 2, we extract the data for the representative summer day previously depicted in Fig. 8 in order to examine the system dispatch.

Fig. 9 demonstrates that $(\mathcal{P})$ and $(\mathcal{S})$ select nearly the same aggregate power dispatch for the 13 SOFCs over the 24-h period. In general, the optimal SOFC power dispatch is the minimum of the aggregate rated power capacity and the building demand

Table 2
Summary of solution differences between $(\mathcal{P})$ and $(\mathcal{S})$ for the *annual* instance of the case study. Each column indicates which formulation is utilized to determine the system design and dispatch.

Annual statistics	$(\mathcal{P})$ Design $(\mathcal{P})$ Dispatch	$(\mathcal{S})$ Design $(\mathcal{S})$ Dispatch	$(\mathcal{S})$ Design $(\mathcal{P})$ Dispatch	$(\mathcal{P})$ Design $(\mathcal{S})$ Dispatch
Total Installed Cost [$]	35,230	29,810	29,810	35,230
SOFC Gas Input [MW h]	2221	2100	2041	2327
Boiler Gas Input [MW h]	2552	2568	2593	2522
Total Utility Gas Cost [$] [a]	160,358	156,828	155,730	162,911
SOFC Power Output [MW h]	953.5	860.9	860.9	953.9
Grid Power Output [MW h]	290.2	382.9	382.9	289.8
Total Utility Power Cost [$] [b]	42,886	54,967	54,967	42,842
SOFC Heat Output [MW h]	461.0	398.9	424.6	442.0
Tank Heat Output [MW h]	331.5	319.6	300.4	354.1
Boiler Heat Output [MW h]	1914	1926	1945	1891
Total O&M Cost [$]	38,211	36,476	36,668	37,993
Total Cost [$]	276,686	278,082	277,175	278,976

[a] The total gas cost includes the taxes paid for the carbon emissions resulting from the combustion of natural gas.
[b] The total power cost includes the taxes paid for the carbon emissions from the grid and the monthly peak demand charges.

Please cite this article in press as: Pruitt KA et al. Evaluating shortfalls in mixed-integer programming approaches for the optimal design and dispatch of distributed generation systems. Appl Energy (2012), http://dx.doi.org/10.1016/j.apenergy.2012.07.030

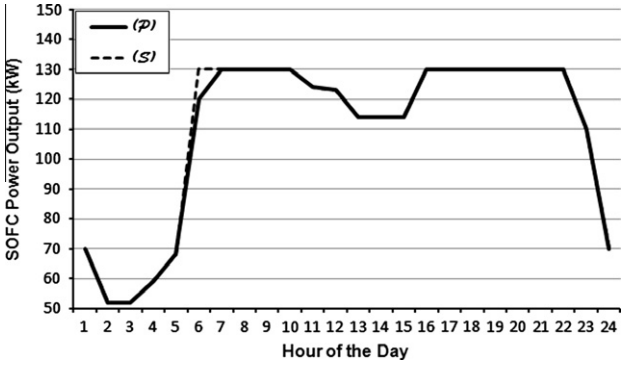

Fig. 9. Optimal SOFC power output as determined by $(\mathcal{P})$ versus $(\mathcal{S})$.

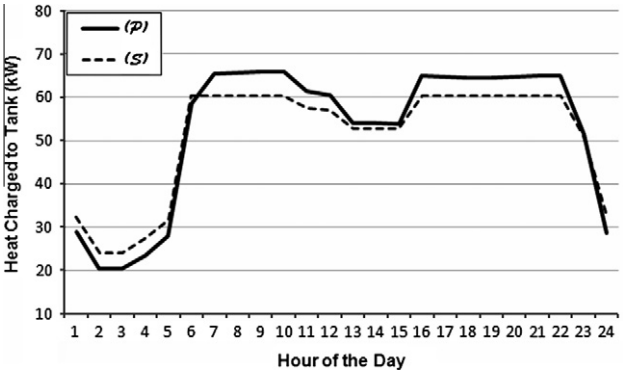

Fig. 11. Optimal SOFC exhaust heat transferred to storage tank as determined by $(\mathcal{P})$ versus $(\mathcal{S})$.

(i.e., $P_{4t} = \min\left(130, d_t^p\right)$). However, there are certain hours throughout the year when the SOFCs are not capable of the ramp up in power output dictated by the building demand. For the day depicted in Fig. 9, the building power demand increases by 80 kW between the fifth and sixth hours. This increase in power demand is beyond the 52 kW total hourly ramping capacity of the 13 SOFCs. The optimal power dispatch determined by $(\mathcal{P})$ appropriately restricts the hourly increase in SOFC power output to 52 kW. By contrast, $(\mathcal{S})$ prescribes an infeasible increase in SOFC power output between the fifth and sixth hours of the day. $(\mathcal{S})$ similarly overestimates the SOFC power output in other hours throughout the year, which accounts for the overestimation of the *annual* SOFC power output compared to $(\mathcal{P})$.

The natural gas consumed by the SOFCs to generate power also differs between the two formulations, as depicted in Fig. 10. As previously predicted in Fig. 5, $(\mathcal{S})$ overestimates the natural gas consumption in any hour in which the SOFCs operate below maximum power output. In fact, in the early hours of the day, $(\mathcal{S})$ overestimates the SOFC gas consumption by as much as 29% compared to $(\mathcal{P})$. The more hours the SOFCs operate at part-load, the more $(\mathcal{S})$ overestimates the fuel requirements for the SOFCs. Because the optimal dispatch strategy in this scenario is load-following and, the SOFCs frequently operate at part-load, $(\mathcal{S})$ overestimates the *annual* SOFC fuel consumption compared to $(\mathcal{P})$.

The overestimation of SOFC fuel requirements by $(\mathcal{S})$ also contributes to differences in the thermal dispatch prescribed by the two formulations. Fig. 11 depicts the optimal exhaust heat dispatch from the SOFCs to the water tank as determined by $(\mathcal{P})$ versus $(\mathcal{S})$. $(\mathcal{S})$ overestimates the heat charged to the tank at low SOFC power output and underestimates it at high SOFC power output (as previously shown in Fig. 6). In the early hours of the day, when SOFC power output is low, $(\mathcal{S})$ overestimates the exhaust heat charged to the storage tank by as much as 19%. In these hours, $(\mathcal{S})$ prescribes an infeasible heat dispatch (i.e., more heat than is actually available) from the SOFCs. During the two peak power demand periods of the day, when SOFC power output is at or near maximum, $(\mathcal{S})$ underestimates the exhaust heat charged to the tank by as much as 9%. The more hours the SOFCs operate at or near rated capacity, the more $(\mathcal{S})$ underestimates the heat that can be generated by the SOFCs. For this scenario, the SOFCs operate at rated capacity in enough hours throughout the year to cause $(\mathcal{S})$ to underestimate the *annual* SOFC heat output compared to $(\mathcal{P})$.

In the description of Fig. 7, we stated that $(\mathcal{S})$ likely underestimates the heat discharged from the storage tank in periods of high heating demand and/or high tank water temperature, and likely overestimates the heat discharge in periods of low heating demand and/or low tank water temperature. Fig. 12 depicts the optimal flowrate and temperature of the tank water as determined by $(\mathcal{P})$. The flowrate of the tank water closely follows the heating demand of the building, while the tank water temperature increases during periods of low demand and decreases during periods of high demand. Fig. 13 demonstrates the impact of the water flowrate and temperature on the tank heat discharge, as determined by $(\mathcal{P})$, and contrasts the prescribed heat discharge with that of $(\mathcal{S})$. During the two peak heating demand periods of the day, $(\mathcal{S})$ underestimates the tank heat discharge by as much as 36%. However, in the middle of the day, when the heating demand is relatively low and the tank water is still well below delivery temperature, $(\mathcal{S})$ overestimates the tank heat discharge by as much as 97%, when compared to $(\mathcal{P})$. In these hours, $(\mathcal{S})$ prescribes an infeasible heat dispatch from the storage tank. Additionally, any hour in which $(\mathcal{S})$ overestimates the heat provided by the storage tank, it underestimates the additional heat that must be provided by the boiler, and thus underestimates the fuel requirements for the boiler. Ultimately, these hourly miscalculations cause $(\mathcal{S})$ to overestimate the *annual* tank heat output, underestimate the *annual* boiler heat output, and underestimate the *annual* boiler fuel input.

For this particular building power load, the aggregate power output of the SOFCs never reaches the maximum turn-down. With 130 kW of rated capacity and a 20% maximum turn-down, the aggregate power output must decrease below 26 kW before any number of SOFCs is forced into standby mode. Because the minimum hourly power load for the year is 52 kW, this particular system does not demonstrate SOFC standby mode or, consequently, SOFC start-up. However, for other simulated load profiles (or in the real-world application of the system) the power demand could fall below the 26 kW threshold. In these cases, the ability to model the effects of SOFC standby and start-up is important.

Interestingly, the cumulative effect of the hourly miscalculations of power, gas, and heat dispatch by $(\mathcal{S})$ is only a slight overestimation of the total annual operational cost, but a more

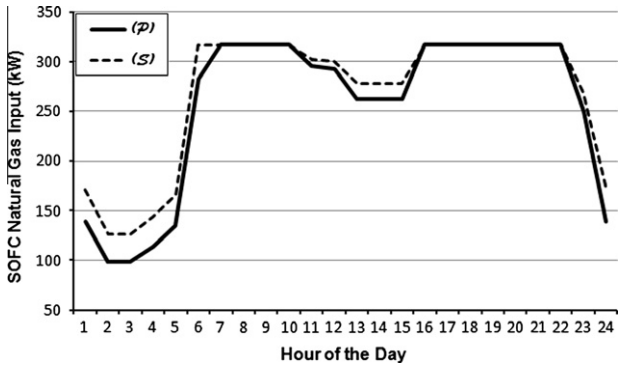

Fig. 10. Optimal SOFC natural gas input as determined by $(\mathcal{P})$ versus $(\mathcal{S})$.

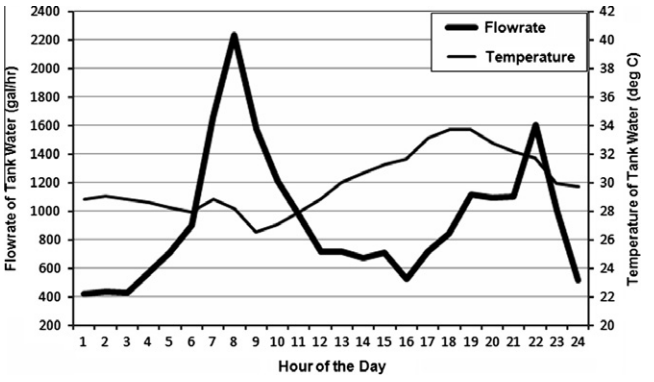

Fig. 12. Optimal storage tank water flowrate and temperature as determined by $(\mathcal{P})$.

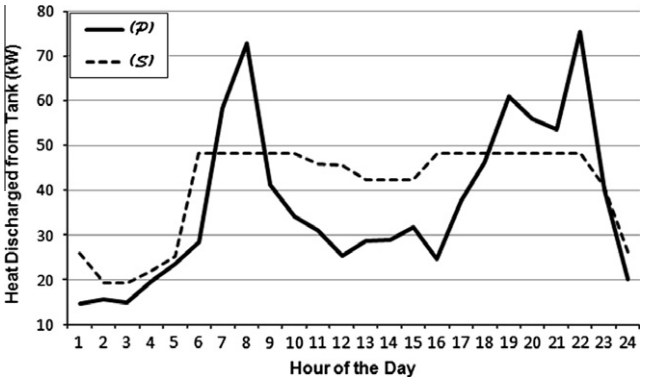

Fig. 13. Optimal storage tank heat dispatch as determined by $(\mathcal{P})$ versus $(\mathcal{S})$.

significant underestimation of the optimal SOFC capacity. In this paper, we demonstrate the miscalculations by $(\mathcal{S})$ for a large hotel located in Wisconsin. However, other locations with similar utility rates, policies, procedures, and emissions produce comparable results. In general, any location with a relatively high electricity-to-gas price ratio, a relatively high rate of carbon emissions, *and* restrictive net-metering policies will result in similar miscalculations by $(\mathcal{S})$. For example, according to EIA reports on state electricity prices, carbon emissions, and natural gas prices (see [33,34]), Indiana, Kentucky, Minnesota, Montana, North Dakota, and Wyoming have energy market conditions similar to those of Wisconsin. These same states also have unfavorable net-metering policies and interconnection procedures for customer-sited DG, according to the NNEC (see [35]). For locations such as these, the $(\mathcal{S})$ formulation is insufficient to accurately determine the optimal design and dispatch of a DG system, and we prefer the more detailed $(\mathcal{P})$ formulation.

5. Conclusions

Extant research approaches the problem of designing and dispatching DG systems with a variety of models and solution techniques. Arguably, the most robust DG system design and dispatch model in the literature is DER-CAM. This MILP model is capable of prescribing a globally minimum total cost mix, capacity, and operational schedule of an assortment of DG technologies. Though simplified models such as DER-CAM allow for the rapid solution of large problem instances, the trade-off for this simplicity is the recommendation of a suboptimal, or even infeasible, system design and dispatch in some instances.

A MINLP formulation of the design and dispatch problem addresses some of the shortfalls in simpler models by considering dynamic (i.e., off-design) performance characteristics of DG technologies. Given the complex and often nonlinear behavior inherent in the operation of real-world systems, a MINLP formulation captures the dynamic performance of CHP and thermal storage technologies more accurately than simpler, linear models. However, the nonlinearities and additional integer variables required to model this behavior render instances of the problem more difficult to solve. Thus, the purpose of this paper is to justify the more complex formulation by demonstrating scenarios for which it is important to model off-design performance and by evaluating the impact on the prescribed design and dispatch of neglecting system dynamics.

In general, off-design performance limitations can be important to consider when the operational schedule of DG technologies is expected to vary over time (e.g., in load-following strategies). Depending on the physical and economic viability of generation and storage technologies, and on the rates, policies, and procedures of local utilities, on-site generator output may be required to follow the load demand during certain time periods. Because load-following requires generators to operate at part-load, ramp power output between time periods, and potentially enter standby mode, the inability to constrain system dynamics could result in an unrealistic dispatch schedule. The off-design operation of CHP technologies also impacts the accurate determination of the thermal energy that can be captured and stored. Ultimately, miscalculations in the operation of the technologies over time could result in the selection of a system with suboptimal capacity.

We numerically demonstrate the effect of neglecting system dynamics via a case study of a large hotel, located in southern Wisconsin, retrofitted with SOFCs and a hot water storage tank. For this example, a simple MILP model overestimates the annual fuel requirements of the SOFCs, underestimates the annual amount of exhaust heat that can be recovered from the SOFCs, overestimates the annual amount of thermal energy available from the tank, and underestimates the annual fuel requirements for the existing heating system. The cumulative impact of these miscalculations is that the MILP overestimates the annual operational costs of the system compared to the MINLP. By overestimating the costs, the MILP underestimates the optimal SOFC capacity by 15%.

Ultimately, the preference for either a MINLP or a MILP formulation of the design and dispatch problem depends on both the purpose of the model and on the primary operating strategy (e.g., load-follow versus baseload) that is expected for the application under study. If the purpose of the model is to employ it as a screening tool to determine which DG technologies are attractive in a given application, then a simple MILP formulation may be adequate. If, however, more detailed engineering analyses of the equipment sizing and system dispatch are the objective, then a higher-fidelity MINLP formulation is more appropriate. Furthermore, simple models of DG technologies under design conditions are sufficient to determine the optimal system acquisition and operation for *some* operating strategies (e.g., when the technologies baseload). However, we demonstrate that strategies exist for which not considering off-design performance can lead to the recommendation of a suboptimal system design. Additionally, a more detailed model permits the observation and analysis of dynamic aspects of technological performance that simpler models cannot capture. Such analyses could reveal desirable performance characteristics of individual DG technologies, and elucidate the impact of those characteristics on the economic viability of integrated DG systems.

Future embellishments to the MINLP model presented here could include the consideration of uncertainty in building demand, market pricing, and system availability. A multi-stage, stochastic programming approach to the design and dispatch problem could

Please cite this article in press as: Pruitt KA et al. Evaluating shortfalls in mixed-integer programming approaches for the optimal design and dispatch of distributed generation systems. Appl Energy (2012), http://dx.doi.org/10.1016/j.apenergy.2012.07.030

identify DG system designs that are robust to changes in the dispatch parameters. However, the introduction of stochasticity increases the complexity of a MINLP problem that is already difficult to solve. As with the research presented here, it would be useful to determine the real-world scenarios for which the added complexity (i.e., uncertainty) is of value.

Acknowledgments

The authors thank the National Science Foundation for partial support of this research effort under award #CNS-0931748. We are also grateful to Andrew Schmidt, Department of Mechanical Engineering, Colorado School of Mines, for providing the building load data from EnergyPlus.

References

[1] Manfren M, Caputo P, Costa G. Paradigm shift in urban energy systems through distributed generation: methods and models. Appl Energy 2011;88:1032–48.
[2] Cotrell J, Pratt W. Modeling the feasibility of using fuel cells and hydrogen internal combustion engines in remote renewable energy systems. NREL/TP-500-34648, National Renewable Energy Laboratory; September 2003.
[3] Givler T, Lilienthal P. Using HOMER software, NRELs micropower optimization model, to explore the role of gen-sets in small solar power systems. NREL/TP-710-36774, National Renewable Energy Laboratory; May 2005.
[4] Khan M, Iqbal M. Pre-feasibility study of stand-alone hybrid energy systems for applications in Newfoundland. Renew Energy 2005;30(6):835–54.
[5] Georgilakis P. State-of-the-art of decision support systems for the choice of renewable energy sources for energy supply in isolated regions. Int J Distribut Energy Resour 2006;2(2):129–50.
[6] Boait P, Rylatt R, Stokes M. Optimisation of consumer benefits from microcombined heat and power. Energy Build 2006;38:981–7.
[7] Medrano M, Brouwer J, McDonell V, Mauzey J, Samuelsen S. Integration of distributed generation systems into generic types of commercial buildings in California. Energy Build 2008;40:537–48.
[8] Mago P, Hueffed A. Evaluation of a turbine driven CCHP system for large office buildings under different operating strategies. Energy Build 2010;42:1628–36.
[9] Nosrat A, Pearce J. Dispatch strategy and model for hybrid photovoltaic and trigeneration power systems. Appl Energy 2011;88:3270–6.
[10] Kong X, Wang R. Energy optimization model for a CCHP system with available gas turbines. Appl Thermal Eng 2005;25:377–91.
[11] Subbaraj P, Rengaraj R, Salivahanan S. Enhancement of combined heat and power economic dispatch using self adaptive real-coded genetic algorithm. Appl Energy 2009;86:915–21.
[12] Burer M, Tanaka K, Favrat D, Yamada K. Multi-criteria optimization of a district cogeneration plant integrating a solid oxide fuel cell-gas turbine combined cycle, heat pumps and chillers. Energy 2003;28:497–518.
[13] Xu D, Kang L, Cao B. The elitist non-dominated sorting GA for multi-objective optimization of standalone hybrid wind/PV power systems. J Appl Sci 2006;6(9):2000–5.
[14] Kayo G, Ooka R. Building energy system optimizations with utilization of waste heat from cogenerations by means of genetic algorithm. Energy Build 2010;42:985–91.
[15] Beihong Z, Weiding L. An optimal sizing method for cogeneration plants. Energy Build 2006;38:189–95.
[16] Weber C, Marechal F, Favrat D, Kraines S. Optimization of an SOFC-based decentralized polygeneration system for providing energy services in an office building in Tokyo. Appl Thermal Eng 2006;26:1409–19.
[17] Oh S, Oh H, Kwak H. Economic evaluation for adoption of cogeneration system. Appl Energy 2007;84:266–78.
[18] Ren H, Gao W. A MILP model for integrated plan and evaluation of distributed energy systems. Appl Energy 2010;87:1001–14.
[19] Ren H, Zhou W, Nakagami K, Gao W, Wu Q. Multi-objective optimization for the operation of distributed energy systems considering economic and environmental aspects. Appl Energy 2010;87:3642–51.
[20] Siddiqui A, Marnay C, Bailey O, LaCommare K. Optimal selection of on-site generation with combined heat and power applications. Int J Distribut Energy Resour 2005;1(1):33–62.
[21] Siddiqui A, Marnay C, Edwards J, Firestone R, Ghosh S, Stadler M. Effects of a carbon tax on microgrid combined heat and power adoption. J Energy Eng 2005;131(1):2–25.
[22] Siddiqui A, Marnay C, Firestone R, Zhou N. Distributed generation with heat recovery and storage. In: LBNL-58630, Lawrence Berkeley National Laboratory; July 2005.
[23] Stadler M, Marnay C, Siddiqui A, Lai J, Aki H. Integrated building energy systems design considering storage technologies. In: LBNL-1752E, Lawrence Berkeley National Laboratory; April 2009.
[24] Pruitt K, Leyffer S, Newman A, Braun R. A mixed-integer nonlinear program for the optimal design and dispatch of distributed generation systems. Optimization and Engineering 2012, submitted for publication.
[25] Stambouli A, Traversa E. Solid oxide fuel cells (SOFCs): a review of an environmentally clean and efficient source of energy. Renew Sustain Energy Rev 2002;6:433–55.
[26] Braun R, Klein S, Reindl D. Evaluation of system configurations for SOFC-based micro-CHP systems in residential applications. J Power Sources 2006;158:1290–305.
[27] Hawkes A, Aguiar P, Hernandez-Aramburo C, Leach M, Brandon N, Green T, et al. Techno-economic modelling of a solid oxide fuel cell stack for micro combined heat and power. J Power Sources 2006;156:321–33.
[28] Braun R. Techno-economic optimal design of SOFC systems for residential micro-combined heat and power applications in the U.S. ASME J Fuel Cell Sci Technol 2010;7:031018:1–15.
[29] Department of Energy. Getting started with EnergyPlus: basic concepts manual information you need about running EnergyPlus, October 2010.
[30] Deru M, Field K, Studer D, Benne K, Griffith B, Torcellini P, et al. US department of energy commercial reference building models of the national building stock. In: NREL/TP-5500-46861, National Renewable Energy Laboratory; February 2011.
[31] Wisconsin Electric Power Company. Electric rates Cg 2, vol. 19; 2011.
[32] Wisconsin Electric-Gas Operations. Firm sales service x-100, vol. 16; 2011.
[33] US Energy Information Administration. State electricity profiles 2010; DOE/EIA-0348(01)/2, January 2012.
[34] US Energy Information Administration. Natural gas annual 2010, DOE/EIA-0131(10), December 2011.
[35] Network for New Energy Choices. Freeing the grid: best and worst practices in state net metering policies and interconnection procedures, December 2010.
[36] Fuel Cell Today. The fuel cell today industry review 2011. Corporate report <www.fuelcelltoday.com>.
[37] DDI Energy Inc. DDI Energy ARC Solid Oxide Fuel Cell (SOFC) electric generation system information. Corporate data sheet, <http://www.ddienergy.ca/home/pricing> [accessed Jun 2012].
[38] Nanjou A. Commercialization of SOFC micro-CHP in the Japanese market. In: Proceedings of the 10th European SOFC forum, Luzern, Switzerland; 26–30 June 2012.
[39] Driscoll D, White B. The status of SOFC programs in USA. In: Proceedings of the 10th European SOFC forum, Luzern, Switzerland; 26–30 June 2012.
[40] International Business Machines. IBM ILOG AMPL version 12.2 user's guide: standard (command-line) version including CPLEX directives, May 2010.
[41] Nakajo A, Mueller F, McLarty D, Brouwer J, Van herle J, Favrat D. The effects of dynamic dispatch on the degradation and lifetime of solid oxide fuel cell systems. J Electrochem Society 2011;158(11):B1329–40.

Please cite this article in press as: Pruitt KA et al. Evaluating shortfalls in mixed-integer programming approaches for the optimal design and dispatch of distributed generation systems. Appl Energy (2012), http://dx.doi.org/10.1016/j.apenergy.2012.07.030